



A comparative numerical study of a semi-infinite heat conductor subject to double strip heating under non-Fourier models

Emad Awad^{1,a} , Mohsen Fayik^{1,b} , Amr R. El-Dhaba^{2,c} 

¹ Department of Mathematics, Faculty of Education, Alexandria University, Souter St. El-Shatby, P.O. box 21526, Alexandria, Egypt

² Department of Mathematics, Faculty of Science, Damamhur University, Damamhur 22511, Egypt

Received: 11 July 2022 / Accepted: 13 November 2022

© The Author(s) 2022

Abstract The present work considers a two-dimensional (2D) heat conduction problem in the semi-infinite domain based on the classical Fourier model and other non-Fourier models, e.g., the Maxwell–Cattaneo–Vernotte (MCV) equation, parabolic, hyperbolic, and modified hyperbolic dual-phase-lag (DPL) equations. Using the integral transform technique, Laplace, and Fourier transforms, we provide a solution of the problem (Green’s function) in Laplace domain. The thermal double-strip problem, allowing the wave interference within the heat conductor, is considered. A numerical technique, based on the Durbin series for inverting Laplace transform and the trapezoidal rule for calculating an integral form of the solution in the double-strip case, is adopted to recover the solution in the physical domain. Finally, discussions for different non-Fourier heat transfer situations are presented. We compare among the speeds of hyperbolic heat transfer models and shed light on the concepts of flux-precedence and temperature-gradient-precedence, *hallmarks* of the lagging response idea. Otherwise, we emphasize the existence of a relationship between the waves speed and the time instant of interference onset, underlying the five employed heat transfer models.

1 Introduction

The classical Fourier law of heat conduction [1] had been and still is the basis of modeling a wide range of engineering and physical applications. In the short-time domain, the heat transfer in specific types of solid conductors tends to behave like a wave rather a diffusion, a phenomenon known as “second sound”, see [2] and the references therein. Hence, the diffusive nature of the Fourier law along the entire temporal scale failed to capture such a wave-like phenomenon, and thus modeling of many heat transfer experiments using Fourier law, in the short-time domain, is questionable and a quantitative modification or an alternative constitutive law should be invoked in such situations. The Maxwell–Cattaneo–Vernotte equation, known also as the telegrapher equation, with its transition from wave to diffusion by including an additional second-order time derivative, is a successful mathematical tool representing a wave with finite speed in the short-time domain and reduces to classical Fourier law in the long-time domain.

With the development of laser-based metal processing, the term “ultrafast/ultrashort laser heating process” was arisen and developed through a string of investigations, see e.g., [3–8]. The ultrafast laser heating process in metals takes place in two steps: The first is the production of hot electron gas in the photon–electron interaction step, and the second is the energy exchange in the electron–phonon collisions, and this process is described through the phenomenological two-temperature model [3]. In [7], the experimental results of Brorson et al. [4] were compared with the numerical results of the two-temperature model and the one-temperature model (based on MCV equation), and they found a good agreement with the two-temperature (known also as two-step) model. The energy equation governing the lattice and the electron temperatures resulting from the two-temperature model is of parabolic type, i.e., it does not behave like a wave with finite speed in the short-time domain (as in the case of classical Fourier law). A hyperbolic two-temperature model was developed and rigorously derived from the Boltzmann transport equation in [8], in which the electron heat flux is relaxed. In both parabolic [7] and hyperbolic [8] two-temperature models, the lattice thermal conductivity is disregarded, which was the cornerstone of the investigation due to Chen and Beraun [9].

The thermal lagging response, with its familiar basic concepts (flux-precedence and temperature-gradient-precedence), was introduced, based on the hypothesis that the instantaneous occurrence between the heat flux and temperature gradient displayed by the classical Fourier law may not be realistic in heat transfer phenomena occurring within the short-time domain. Instead, the

This work is dedicated to Professor Hany H. Sherief on the occasion of his 73rd birthday.

^a e-mail: emadawad78@alexu.edu.eg

^b e-mail: m_fayik@alexu.edu.eg

^c e-mail: a.r.eldhaba@sci.dmu.edu.eg (corresponding author)

non-instantaneous response shown by the SPL, or the DPL constitutive laws was assumed, see Eq. (3), and refer to the comprehensive latest monograph [10]. The DPL constitutive law derives its importance from the fact that its first approximation (known as Jeffreys-type constitutive law) yields a temperature representation coinciding well with its counterpart that governs the electron and the lattice temperatures in the parabolic two-temperature model and the lattice temperature resulting from the Guyer–Krumhansl model [11]. We refer the reader to the work [12] for other perspectives on the hyperbolic DPL model and its matching with the hyperbolic two-temperature model. In [13], Jou and Criado-Sancho showed the conditional thermodynamic stability of the parabolic DPL model with bounded initial condition for the temperature time-rate and they provided a thermodynamical derivation for the parabolic DPL from the extended entropy including the heat flux and the flux of heat flux. On the other hand, Serdyukov [14] studied the derivability of the parabolic DPL equation by assuming that the entropy is a function of the internal energy density and its first and second time rates. Xu [15], based on the postulates of the works [13] and [14], showed that the general form of the DPL or SPL equations can be compatible with the second law of thermodynamics, refer to [10, 12] for further generalizations. From a mathematical point of view, the parabolic DPL equation and its higher order approximations were showed to satisfy the stability criteria, well-posedness and spatial decay estimates under certain limitations on the DPL coefficients by Quintanilla and Rack [16, 17]. Furthermore, the generalized variational principles for the Fourier, MCV, parabolic DPL, two-temperature, and Guyer–Krumhansl heat conduction models have been obtained using the Laplace transform and employed to approximate analyses based on the Rayleigh–Ritz method by Li and Cao [18, 19]. We refer the reader to the recent works on the MCV telegraph equation and its generalizations which have investigated its connection with continuous-time random walk scheme and its conditional solutions [20, 21], the Doppler effect [22], and the integral decomposition [23].

Despite its conditional consistency with the second law of thermodynamics, inspiring from the criticism on the Maxwell–Cattaneo–Vernotte (or the telegrapher) equation [24, 25], Rukolaine [26, 27] found an unphysical effect of the parabolic and hyperbolic DPL equations by exhibiting negative values for the temperature in higher dimensions when the (non-negative) Dirac delta function is considered as an initial condition. Rukolaine investigation was carried out on an infinite three-dimensional space. Recently, the work [28] has shed light on the Rukolaine finding and set the sufficient conditions for the parabolic DPL equation to satisfy the non-negativity criteria in all dimensions. Most recently, the parabolic DPL equation has been derived from the continuous-time random walk (CTRW) scheme [29] provided that the sufficient conditions suggested in [28] are met. In addition, many applications in anomalous diffusion, e.g., the cage effect, retarded and accelerated subdiffusion, and the crossover from superdiffusion to subdiffusion, have been found to be successfully described by the generalized “fractional” DPL equation with flux-precedence (or flux-driven), see also [30].

The one-dimensional formulation of the parabolic and hyperbolic DPL heat conduction was provided by Tzou in finite domain [11] and semi-infinite domain [31]. The multi-dimensional Green’s function of the DPL model was formulated in [32] with a one-dimensional example on thin plate. Most recently, the one- and two-dimensional Green’s functions for the parabolic DPL in [33] are analytically solved; in addition, they found a good agreements with the experimental results [4] and [34]. Furthermore, we mention the 3D formulation of the parabolic DPL model [35] wherein a 3D schematic for laser heating of a gold film was provided. The rectangular two-dimensional formulation of the parabolic DPL model in thin plates of single-layer was studied in [36] and of single and double layer in [37]. The axisymmetric formulation in terms of the cylindrical polar coordinates was discussed also by Han et al. [36] for single-layer circular plate and [38] for a functionally graded cylinder. We refer also to some works of Dai and coworkers on the DPL heat conduction model and the two-step model, using different dimensions and numerical schemes [39–41].

The current work aims to introduce a visualization of the thermal propagation within a rigid semi-infinite conductor induced by exponentially decaying double-strip surface heating, by using different governing models expressing various theories of heat transfer mechanisms. We use an integral technique based on Laplace–Fourier transform to simplify the problem to a solution of a simple ordinary differential equation, then we use numerical techniques based on the Durbin series and the trapezoidal rule to recover the solution numerically to the real domain. Some analytical and semi-analytical solutions are provided. We organize the paper as follows: In Sect. 2, we revise on the mathematical foundations of the DPL models and formulate the two-dimensional problem. The Green’s function in the Laplace domain and a semi-analytical solution for the thermal propagation of the double-strip application are derived in Sect. 3. We invert the integral transforms and provide the graphical representations with discussion in Sect. 4. Finally, we give a summary of the work in Sect. 5.

2 Problem formulation

Jeffreys-type heat conduction equation consists of the Jeffreys-type constitutive law [42, 43]:

$$\left(1 + \tau_q \frac{\partial}{\partial t}\right) \mathbf{q}(\mathbf{r}, t) = -k \left(1 + \tau_\theta \frac{\partial}{\partial t}\right) \nabla \theta(\mathbf{r}, t), \quad (1)$$

and the energy balance equation (without volumetric heat sources)

$$-\nabla \cdot \mathbf{q}(\mathbf{r}, t) = C \frac{\partial \theta(\mathbf{r}, t)}{\partial t}. \quad (2)$$

Here, $\theta(\mathbf{r}, t) = T(\mathbf{r}, t) - T_0$, $T(\mathbf{r}, t)$ is the absolute temperature, T_0 is the reference temperature, $\mathbf{q}(\mathbf{r}, t)$ is the heat flux vector, t is the temporal variable, $\mathbf{r} = \langle x, y, z \rangle$ is the position vector, x, y , and z are the Cartesian coordinates and ∇ is the Del operator. In addition, k is the thermal conductivity, C is the heat capacity, and τ_q and τ_θ are time constants. After Tzou hypothesis, the time constants τ_q and τ_θ were interpreted as phase lags in heat flux and temperature gradient, respectively, by replacing the classical Fourier law with the universal “Tzou” constitutive law [10]:

$$\mathbf{q}(\mathbf{r}, t + \tau_q) = -k\nabla\theta(\mathbf{r}, t + \tau_\theta). \tag{3}$$

On the basis that τ_q and τ_θ are small enough, Eq. (3) reduces to (1) in the Taylor’s series approximation. In the case that the orders of τ_q and τ_θ allow us to truncate the Taylor’s series expansion at the second term in the left-hand side and the first term in the right-hand side of Eq. (3), we obtain [31]

$$\left(1 + \tau_q \frac{\partial}{\partial t} + \frac{\tau_q^2}{2} \frac{\partial^2}{\partial t^2}\right) \mathbf{q}(\mathbf{r}, t) = -k \left(1 + \tau_\theta \frac{\partial}{\partial t}\right) \nabla\theta(\mathbf{r}, t), \tag{4}$$

which introduces a hyperbolic heat transfer model coinciding the hyperbolic two-temperature model. An aspect, was suggested in [12], rearranges parameters of the hyperbolic model (4) to

$$\left(1 + \tau_q \frac{\partial}{\partial t} + \tau_m^2 \frac{\partial^2}{\partial t^2}\right) \mathbf{q}(\mathbf{r}, t) = -k \left(1 + \tau_\theta \frac{\partial}{\partial t}\right) \nabla\theta(\mathbf{r}, t), \tag{5}$$

where

$$\tau_q = \tau_{q1} + \tau_{q2}, \quad \tau_m = \sqrt{\tau_{q1}\tau_{q2}}, \tag{6}$$

and τ_{q1} and τ_{q2} are successive phase lags in the heat flux. It is claimed that the modified hyperbolic DPL model (5) with its parameters (6) fits the hyperbolic two-step model [8] better than original hyperbolic version of the DPL (4).

We consider a semi-infinite heat conductor ($x > 0$) with a smooth infinite boundary plane ($x = 0$) subjected to the thermal boundary condition

$$\theta(0, y, z, t) = \Theta(y, t). \tag{7}$$

where $\Theta(y, t)$ is a function of y and t . In order to generate a two-dimensional thermal propagation within the medium, we choose $\Theta(y, t)$ on the form

$$\Theta(y, t) = \Theta_0 f\left(\frac{t}{\tau_q}\right) \delta(y), \tag{8}$$

where $\delta(\cdot)$ is the Dirac delta function and Θ_0 is a constant of dimension *Kelvin* \times *Length*, which represents a thermal line along z -axis varying with time according to the temporal function $f(t)$. By these settings, the temperature and the heat flux are functions of x, y and t , and the Green’s function of temperature [44] can be derived in the Laplace domain as we shall see in the next section.

In the two-dimensional setting, for the sake of comparisons, we rewrite the governing equations including all the above heat transfer models in terms of the rectangular coordinates at the form:

$$\left(1 + \tau_q \frac{\partial}{\partial t} + n_0 \frac{\tau_q^2}{2} \frac{\partial^2}{\partial t^2} + n_1 \tau_m^2 \frac{\partial^2}{\partial t^2}\right) q_x(x, y, t) = -k \left(1 + \tau_\theta \frac{\partial}{\partial t}\right) \frac{\partial\theta(x, y, t)}{\partial x}, \tag{9}$$

$$\left(1 + \tau_q \frac{\partial}{\partial t} + n_0 \frac{\tau_q^2}{2} \frac{\partial^2}{\partial t^2} + n_1 \tau_m^2 \frac{\partial^2}{\partial t^2}\right) q_y(x, y, t) = -k \left(1 + \tau_\theta \frac{\partial}{\partial t}\right) \frac{\partial\theta(x, y, t)}{\partial y}, \tag{10}$$

$$-\frac{\partial q_x(x, y, t)}{\partial x} - \frac{\partial q_y(x, y, t)}{\partial y} = C \frac{\partial\theta(x, y, t)}{\partial t}, \tag{11}$$

subject to the initial conditions

$$q_x(x, y, 0) = 0, q_y(x, y, 0) = 0, \theta(x, y, 0) = 0, \tag{12}$$

and the boundary condition (8). In Eqs. (9) and (10), we have combined the original and the modified models of hyperbolic DPL by introducing the integer numbers which take their values from the set $\{0, 1\}$. Introducing the following non-dimensional transformations and quantities:

$$\frac{t}{\tau_q} \rightarrow t, \quad \frac{x}{\sqrt{\alpha_T \tau_q}} \rightarrow x, \quad \frac{y}{\sqrt{\alpha_T \tau_q}} \rightarrow y, \quad \frac{\theta}{T_0} \rightarrow \theta, \quad \frac{\Theta}{T_0} \rightarrow \Theta, \quad q \sqrt{\frac{\tau_q}{CkT_0^2}} \rightarrow q, \quad \chi_0 = \frac{\tau_\theta}{\tau_q}, \quad \chi_1 = \frac{\tau_m}{\tau_q}, \tag{13}$$

where $\alpha_T = k/C$ is the thermal diffusivity, we obtain the dimensionless governing equations:

$$\left[1 + \frac{\partial}{\partial t} + \left(\frac{n_0}{2} + n_1 \chi_1^2\right) \frac{\partial^2}{\partial t^2}\right] q_x(x, y, t) = -\left(1 + \chi_0 \frac{\partial}{\partial t}\right) \frac{\partial\theta(x, y, t)}{\partial x}, \tag{14}$$

$$\left[1 + \frac{\partial}{\partial t} + \left(\frac{n_0}{2} + n_1 \chi_1^2 \right) \frac{\partial^2}{\partial t^2} \right] q_y(x, y, t) = - \left(1 + \chi_0 \frac{\partial}{\partial t} \right) \frac{\partial \theta(x, y, t)}{\partial y}, \tag{15}$$

$$- \frac{\partial q_x(x, y, t)}{\partial x} - \frac{\partial q_y(x, y, t)}{\partial y} = \frac{\partial \theta(x, y, t)}{\partial t}, \tag{16}$$

subject to the same homogeneous initial conditions (12) and the dimensionless boundary condition

$$\theta(0, y, t) = f(t)\delta(y), \tag{17}$$

where we have chosen $\Theta_0 = T_0 \sqrt{\alpha_T \tau_q}$.

3 Thermal double-strip application

In this section, we derive the Green’s function of the two-dimensional non-Fourier thermal propagation, governed by (14)–(16), within a semi-infinite heat conductor in terms of the Laplace parameter. We define the one-sided Laplace transform of a generic function $f(x, y, t)$ as [45]

$$\tilde{f}(x, y, s) = \mathcal{L}\{f(x, y, t); t\}(x, y, s) = \int_0^\infty f(x, y, t) \exp(-st) dt, \tag{18}$$

and the Fourier transform of $f(x, y, t)$ as

$$\hat{f}(x, \kappa, t) = \mathcal{F}\{f(x, y, t); y\}(x, \kappa, t) = \int_{-\infty}^\infty f(x, y, t) \exp(i\kappa y) dy. \tag{19}$$

Employing the Laplace–Fourier transform (18) and (19), the generalized governing Eqs. (14)–(16) subject to the zero initial conditions (12) and the boundary condition (17) can be written as a simple homogeneous differential equation:

$$\frac{d^2 \hat{\theta}(x; \kappa, s)}{dx^2} = m^2(\kappa, s) \hat{\theta}(x; \kappa, s), \tag{20}$$

where $m(\kappa, s)$ is given as

$$m(\kappa, s) = \sqrt{\xi^2(s) + \kappa^2} \tag{21}$$

and $\xi(s)$ is given by

$$\xi(s) = \sqrt{\frac{s \left[1 + s + \left(\frac{n_0}{2} + n_1 \chi_1^2 \right) s^2 \right]}{1 + \chi_0 s}}. \tag{22}$$

The solution of (20) can be straightforwardly obtained for semi-infinite heat conductors subject to the boundary condition (17) in the form

$$\hat{\theta}_G(x; \kappa, s) = \tilde{f}(s) \exp(-mx), \tag{23}$$

where $\tilde{f}(s)$ is the Laplace transform of the temporal profile of the boundary condition, $f(t)$. Equation (23) results in the two-dimensional Green’s function in semi-infinite domains. For more discussions about the formulation and solution of Green’s function in the semi-infinite bodies, refer to p. 211 in [44].

Inverting the Fourier transform of the Green’s function (23), we obtain

$$\tilde{\theta}_G(x, y; s) = \frac{1}{\pi} \tilde{f}(s) \int_0^\infty \exp(-x\sqrt{\xi^2(s) + \kappa^2}) \cos(\kappa y) d\kappa. \tag{24}$$

Using the tabulated integrals, we have that

$$\int_0^\infty \exp(-\beta\sqrt{\alpha^2 + \kappa^2}) \cos(\kappa y) d\kappa = \frac{\alpha\beta}{\sqrt{y^2 + \beta^2}} K_1 \left(\alpha\sqrt{y^2 + \beta^2} \right),$$

for $\Re\{\alpha\} > 0$ and $\beta > 0$, where $K_\nu(\cdot)$ is modified Bessel function of second kind and order ν . Therefore, we get the two-dimensional Green’s function in the Laplace domain

$$\tilde{\theta}_G(x, y; s) = \frac{\xi(s)\tilde{f}(s)x}{\pi\sqrt{x^2 + y^2}} K_1 \left(\xi(s)\sqrt{x^2 + y^2} \right). \tag{25}$$

Similar mathematical formulation and methodology were discussed in [46] for micropolar fluid. Inverting Laplace transform of Eq. (25) analytically is problematic. Here we derive a closed-form of the Green’s function for a very special case in which the

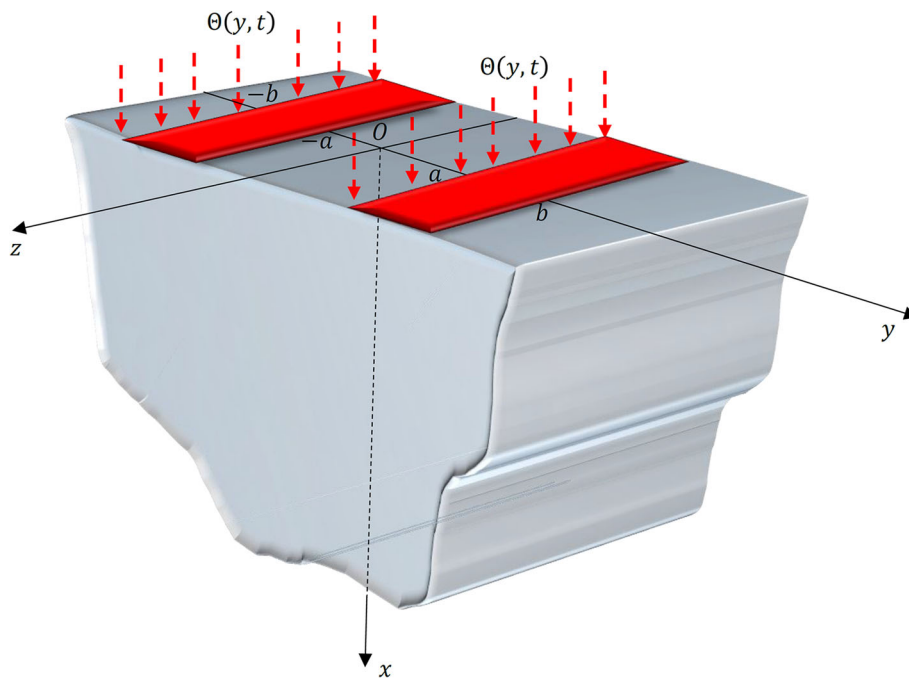


Fig. 1 Problem description

temporal profile of the boundary condition is described through the Heaviside step function $H(t)$ and the Fourier heat transfer is the dominant. In other words, by setting $\xi(s) = \sqrt{s}$ and $\tilde{f}(s) = 1/s$, Eq. (25) reads

$$\tilde{\theta}_{FG}(x, y; s) = \frac{x}{\pi \sqrt{s} \sqrt{x^2 + y^2}} K_1\left(\sqrt{s} \sqrt{x^2 + y^2}\right), \tag{26}$$

where the subscript FG refers to the Green’s function of the Fourier law in the half-space when the temporal profile of the boundary condition is the Heaviside unit step. Using the tabulated rule [45]

$$\mathcal{L}^{-1}\left\{\frac{1}{\sqrt{s}} K_1(\sqrt{\alpha s})\right\} = \frac{1}{\sqrt{\alpha}} \exp\left(-\frac{\alpha}{4t}\right),$$

Equation (26) yields

$$\theta_{FG}(x, y, t) = \frac{x}{\pi(x^2 + y^2)} \exp\left(-\frac{1}{4t} \sqrt{x^2 + y^2}\right). \tag{27}$$

In the end of this section, we apply the derived 2D Green’s function (25) on the double-strip problem, refer to the problem description in Fig. 1, see also p. 223 in [44] for a variety of formulations. We further assume an exponential decay for the temporal profile of the boundary condition. In other words, the dimensionless boundary condition that replaces (17) is given as

$$\theta(0, y, t) = \Theta(y, t) = H(t) \exp(-t)[H(|y| - a) - H(|y| - b)], \tag{28}$$

where $a < b$. It is clear from (28) that the temporal profile in Laplace domain has the form $\tilde{f}(s) = 1/(1 + s)$. Thereby, the spatiotemporal distribution of the temperature within the semi-infinite conductor due to the double-strip boundary (28) can be written in the integral form:

$$\theta(x, y, t) = \int_{y+a}^{y+b} \theta_G(x, \zeta, t) d\zeta + \int_{y-b}^{y-a} \theta_G(x, \zeta, t) d\zeta, \tag{29}$$

where the Green’s function in this case, $\theta_G(x, y, t)$, is given in Laplace space as

$$\tilde{\theta}_G(x, y; s) = \frac{\xi(s)x}{\pi(s + 1)\sqrt{x^2 + y^2}} K_1\left(\xi(s)\sqrt{x^2 + y^2}\right), \tag{30}$$

and $\xi(s)$ is given by (22).

4 Numerical results and discussion

In this section, we use two numerical techniques to bring the solution (29)–(30) to the real domain. At first, we invert Laplace transform by employing the Durbin series [10, 28, 47, 48]

$$\begin{aligned} \theta(x, y, t) = & \frac{2 \exp(\gamma t)}{T_1} \left\{ -\frac{1}{2} \tilde{\theta}(x, y, \gamma) \right. \\ & + \Re \left[\sum_{l=0}^{N\text{Sum}} \tilde{\theta} \left(x, y, \gamma + \frac{2\pi i l}{T_1} \right) \cos \left(\frac{2\pi l t}{T_1} \right) \right] \\ & \left. - \Im \left[\sum_{l=0}^{N\text{Sum}} \tilde{\theta} \left(x, y, \gamma + \frac{2\pi i l}{T_1} \right) \sin \left(\frac{2\pi l t}{T_1} \right) \right] \right\} \end{aligned} \quad (31)$$

where $\gamma t \cong 4.7 - 10$, T_1 is chosen so that $0 < t \leq 2T_1$ and the number of summed terms “ $N\text{Sum}$ ” ranges from 10^5 to 10^7 . For accelerating the convergence of the series (31), a subroutine has been prepared using FORTRAN, based on [49]. The method has been successfully employed to invert Laplace transform in a variety of rectangular two-dimensional formulations, see e.g. [50–53]. Since the integration in Eq. (29) could not be implemented analytically, we invoke the trapezoidal rule [54]. We have set $a = 1$ and $b = 3$ in Eq. (28). We represent our numerical results graphically using MATLAB.

The solution (29)–(30) includes six heat transfer models:

- (i) When $n_0 = n_1 = 0$ and $\chi_0 = 1$, the solution (29)–(30) results in the temperature variation of the semi-infinite heat conductor governed by the classical Fourier law.
- (ii) When $n_0 = n_1 = 0$ and $\chi_0 = 0$, we get the temperature distribution governed by the Cattaneo, Maxwell–Cattaneo–Vernotte (telegrapher), or Single-Phase-Lag (SPL) equation of heat transfer.
- (iii) When $n_0 = n_1 = 0$ and $0 < \chi_0 < 1$, we have the parabolic DPL heat transfer model with temperature-gradient precedence.
- (iv) When $n_0 = n_1 = 0$ and $\chi_0 > 1$, we get the half-space solution of the parabolic DPL model with flux-precedence.
- (v) When $n_0 = 1, n_1 = 0$ and $\chi_0 > 1$, we obtain the half-space solution of the hyperbolic DPL [31].
- (vi) When $n_0 = 0, n_1 = 1, \chi_0 > 1$ and $0 < \chi_1 < 1$, we obtain the half-space solution of the modified hyperbolic DPL. It is found that for copper the ratio $\chi_1 = 0.246$ [12], which yields that $\chi_1^2 = 0.06$ not 0.5 as in the original hyperbolic DPL, refer to (22).

In Fig. 2, we show the thermal propagation within an arbitrary semi-infinite medium governed by classical Fourier law, i.e., the case $n_0 = n_1 = 0$ and $\chi_0 = 1$ in which there is an instantaneous response between the heat flux and the temperature gradient. The absence of wavefront characteristic is clear in Fourier diffusion, especially in the short-time response. Because of what-so-called infinite wave speed in Fourier thermal propagation, one can see the beginning of collision between the two waves, coming from the two strips, after dimensionless time $t = 1$. At dimensionless time $t = 10$, the two thermal waves due to the decaying double-strip boundary merge to constitute a single thermal wave propagating within the semi-infinite heat conductor.

Figure 3 exhibits the thermal propagation within the semi-infinite conductor governed by MCV equation. The finite wave speed is clear during the short- and intermediate-time response. The wavefront exists always at $x = t$ because the dimensionless transformation (13) made the thermal waves speed to equal unity (i.e., $v_{MCV} = x/t = 1$). In the relatively long-time response, it is known that the MCV equation loses its feature (finite wave speed) and reduces to the Fourier equation of heat conduction, thereby, the long-time response of MCV coincides its correspondence in Fig. 2e, f. Also, the finite wave speed delays the wave interference between the two waves resulting from the double-strip surface heating, refer to Fig. 3b, in contrast to what occurred in Fourier thermal propagation, refer to Fig. 2b.

In the context of the lagging response, we have that the MCV constitutive law is a temperature-gradient-precedence with finite wave speed [10]. The DPL model with $0 < \chi_0 < 1$ (or $\tau_q > \tau_\theta$) provides a generalized temperature-gradient-precedence situation in which the finite wave speed feature disappears. As expected, one can see the resemblance between the different responses in Figs. 3 and 4 at the four dimensionless instants $t = 0.1, 1, 5$ and 10. The major difference between the two figures is absence of the plane wavefront in the generalized temperature-gradient-precedence situation with $0 < \chi_0 < 1$, and exceedance the limit $x = t$ in all cases. On the other hand, we present the flux-precedence situation ($\chi_0 > 1$) in Fig. 5. Hyper-diffusion nature of the flux-precedence heat transfer situation is clear. In addition, the delayed temperature gradient, characterizes this type of heat flow, brings the peak value very close to the boundary surface, see panel (c) at $t = 5$. This case contradicts entirely the case of pure temperature-gradient-precedence shown in Fig. 3c, i.e., the case of MCV equation. In Figs. 3, 4, and 5, we have omitted the long-time contours of the MCV and DPL based on the fact that all these laws reduce to the Fourier law in the long-time behavior.

In Figs. 6 and 7, we represent the 2D thermal wave governed by the hyperbolic DPL and the modified hyperbolic DPL, respectively. We plot the hyperbolic DPL at two instants $t = 0.1$ and $t = 1$. As the time goes on, the hyperbolic DPL reduces to the parabolic DPL model. On the other hand, we plot the modified hyperbolic DPL at two instants $t = 0.01$ and $t = 0.1$. We found that the modified hyperbolic DPL at $t = 1$ resembles to a great extent the parabolic DPL and the finite speed of thermal waves breaks down. At the time instant $t = 0.1$, we note that the thermal waves governed by three hyperbolic models (MCV, hyperbolic DPL and modified hyperbolic DPL) have plane wavefronts at different positions. The MCV thermal wave cuts xy -plane at $x = 0.1$, the hyperbolic

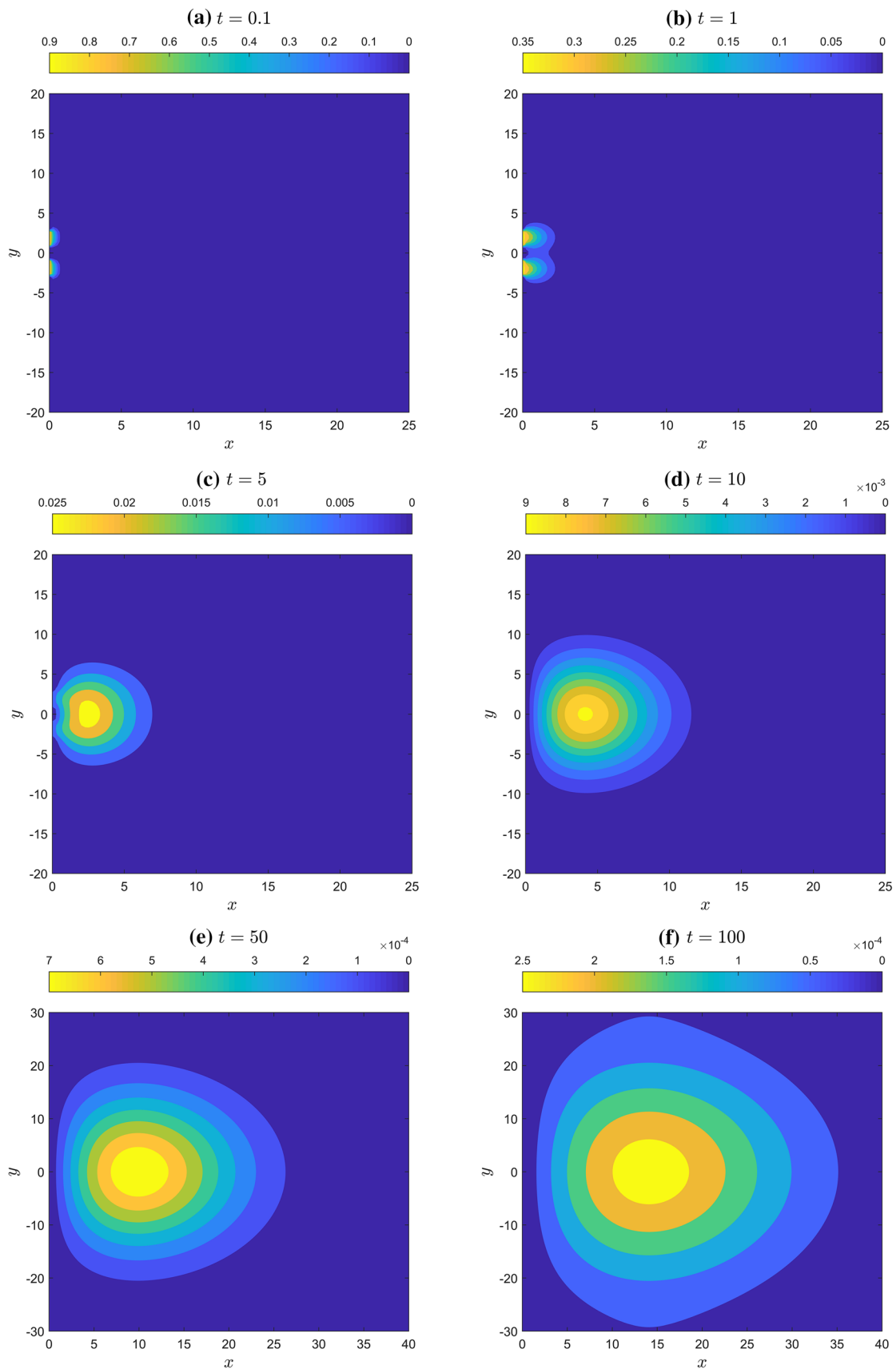


Fig. 2 Two-dimensional thermal propagation with Fourier law at different values of time

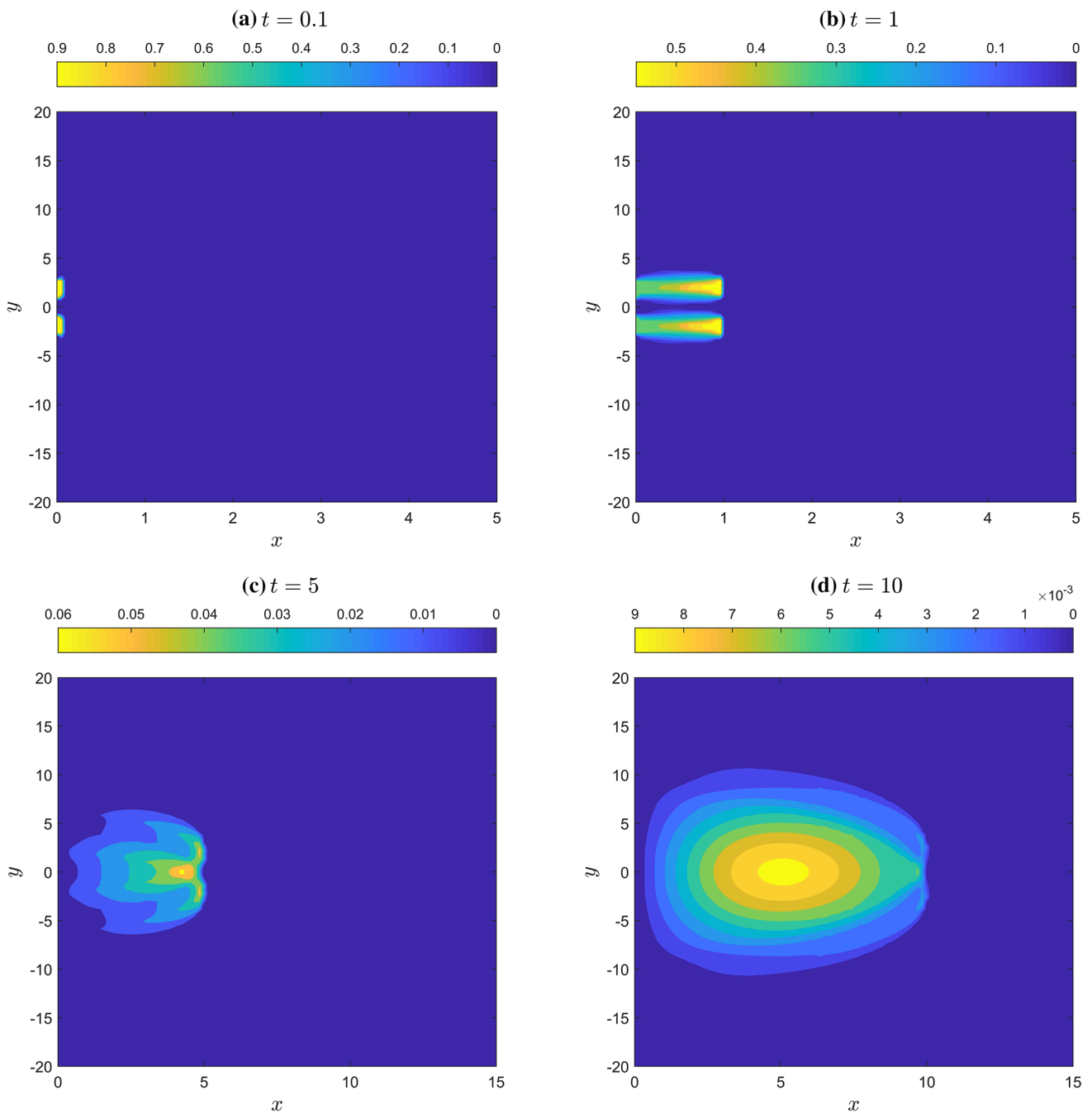


Fig. 3 Two-dimensional thermal propagation with Maxwell–Cattaneo–Vernotte equation at different values of time

DPL thermal wave cuts xy -plane at $x = 0.447$ and the modified hyperbolic DPL thermal wave owns a vertical plane wavefront at $x = 1.412$. Indeed, we have that the MCV wave speed is given as

$$v_{MCV} = \sqrt{\frac{\alpha_T}{\tau_q}}, \tag{32}$$

while the speed of thermal waves governed by the original DPL model is

$$v_{DPL} = \sqrt{\frac{2\alpha_T \tau_\theta}{\tau_q^2}} = \sqrt{2\chi_0} v_{MCV}, \tag{33}$$

and the speed of thermal waves governed by the modified hyperbolic DPL is determined through the relation [12]

$$v_{MDPL} = \sqrt{\frac{\alpha_T \tau_\theta}{\tau_{q1} \tau_{q2}}} = \frac{1}{\sqrt{2}\chi_1} v_{DPL} = \frac{\sqrt{\chi_0}}{\chi_1} v_{MCV}. \tag{34}$$

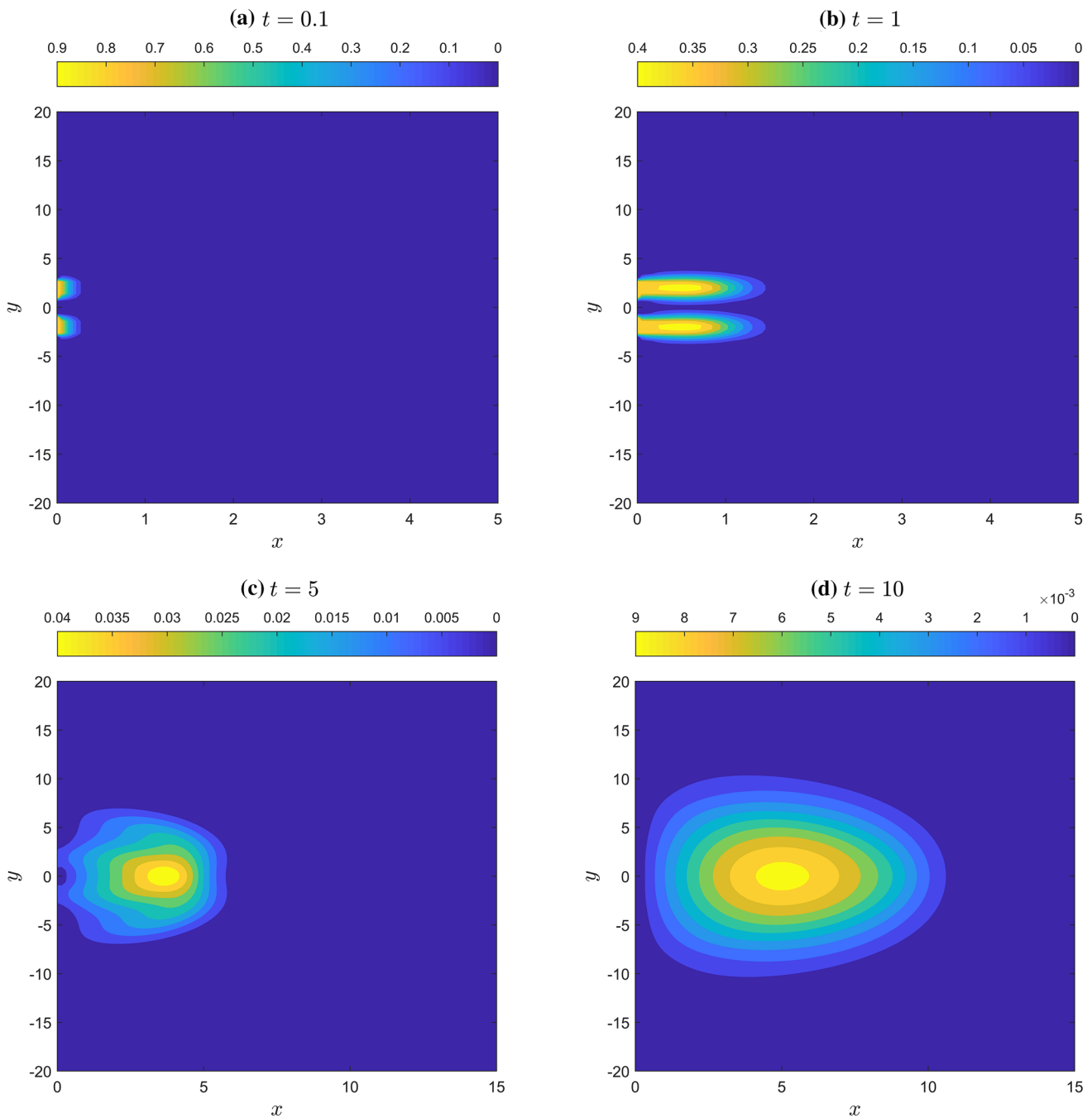


Fig. 4 Two-dimensional thermal propagation with parabolic DPL heat conduction law, when the temperature-gradient-precedence is considered, at different values of time and $\chi_0 = 0.1$

Therefore, if we set $v_{MCV} = 1$, $\chi_0 = 10$ and $\chi_1 = 0.225$, then the plane wavefront of the MCV model cuts xy -plane at $x = t$, the one resulting from the original hyperbolic DPL at $x = 4.47t$ and the modified hyperbolic DPL at $x = 14.117t$. Furthermore, one can conclude from (32)–(34) that if $\chi_0 > 1$ and $\chi_1 < \sqrt{0.5}$, then

$$v_{MDPL} > v_{DPL} > v_{MCV}, \tag{35}$$

i.e., the hyperbolicity of the modified hyperbolic DPL model is activated in a time domain shorter than the domain in which the hyperbolicity of the original hyperbolic DPL model works. The same feature holds true if we compare the original hyperbolic DPL and the hyperbolic MCV model. We refer the reader’s attention to the work [55] wherein a comparison between the velocities of thermal wave computed from the Monte Carlo simulations and the MCV model, for ultra-short laser pulse heating, was carried out. It is salient that the macroscopic MCV model underestimates the thermal wave speed in the ultrafast transient processes, where

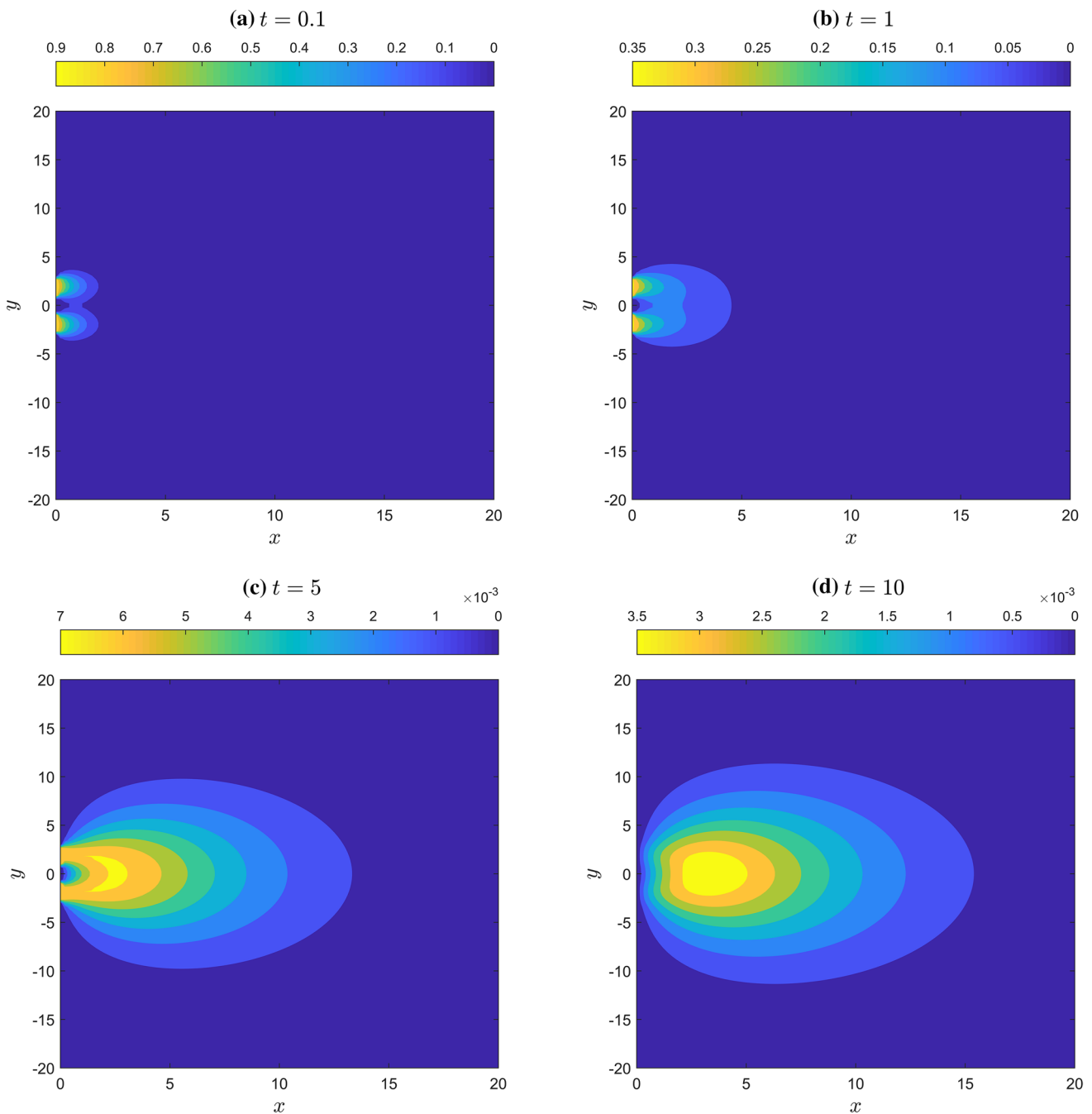


Fig. 5 Two-dimensional thermal propagation with parabolic DPL heat conduction law, when flux-precedence is considered, at different values of time and $\chi_0 = 10$

it predicts a speed equal $\sqrt{3}/3$ of (or less than) the Monte Carlo simulations speed using different phonon emissions (Lambert emission and directional emission), *cf.* Equations (34)–(35).

In Fig. 8, we study the effect of the characteristic ratio χ_0 on the propagation of thermal waves inside the medium. Starting from the subplot (b) of Fig. 5 drawn at the dimensionless time $t = 1$ and the ratio $\chi_0 = 10$, we have increased the value χ_0 to take the multiples 100, 1000 and 10000. As χ_0 increases, we note that thermal effects reach to deeper regions inside the medium with low temperature values, meanwhile, the highest temperature peaks preserve their positions near the thermal boundary. This observation can be verified for other temporal values. Indeed, the large values of χ_0 , i.e., $\chi_0 \gg 1$, means that $\tau_\theta \gg \tau_q$, which indicates to too early heat flux and too late temperature gradient. Therefore, this early heat flux helps the temperature to affect deeper points of the heat conductor without significant temperature variation. Moreover, we note that as $\chi_0 \geq 1000$, the variation of the propagation depth of the thermal wave becomes slower. This is not surprising, because it has been proved that as $\chi_0 \rightarrow \infty$ the temporal change of

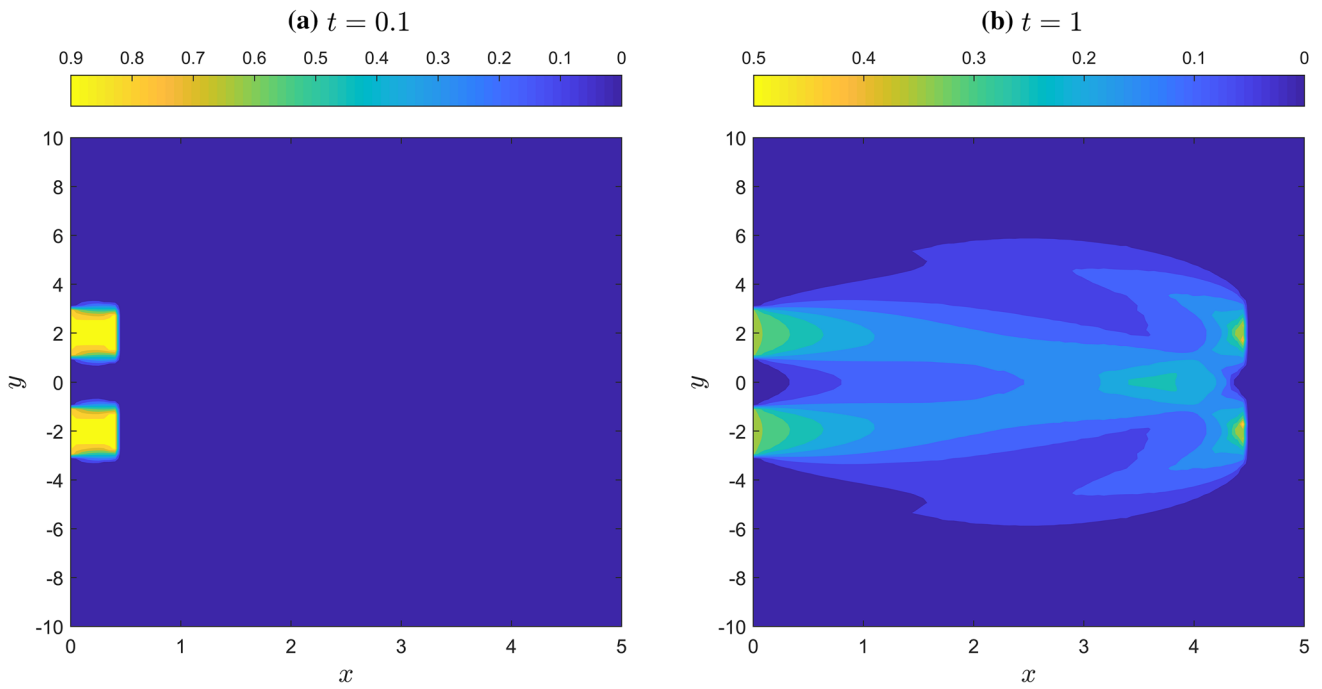


Fig. 6 Two-dimensional thermal propagation with original hyperbolic DPL heat conduction law at different values of time, $n_0 = 1, n_1 = 0$ and $\chi_0 = 10$

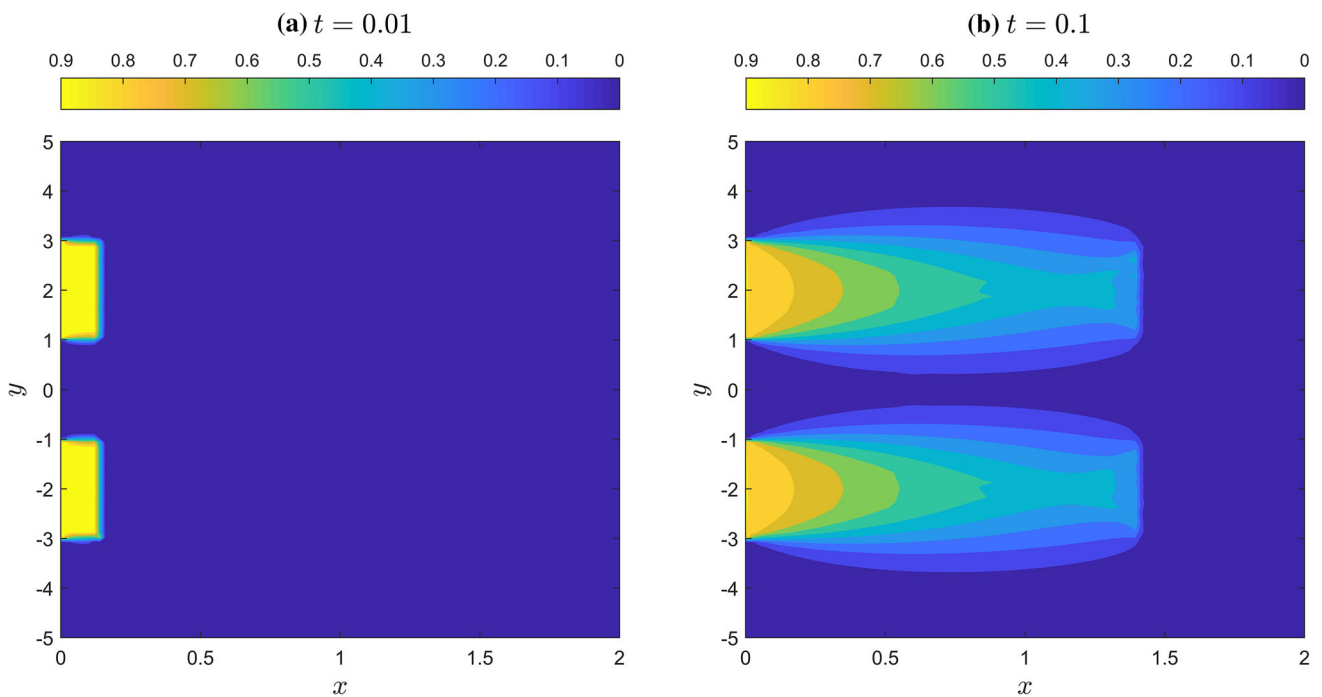


Fig. 7 Two-dimensional thermal propagation with modified hyperbolic DPL heat conduction law at different values of time, $n_0 = 0, n_1 = 1, \chi_1 = 0.225$ and $\chi_0 = 10$

MSD of the distribution becomes zero, i.e., cage-like effect, refer to the fifth figure of [29], or it represents a case of immobilization [56]. It is noteworthy that the situation $\chi_0 \rightarrow \infty$ is the opposite thermal situation to the pure MCV represented in Fig. 3b. Again, one can readily observe the effect of finite wave speed on the time instant of interference onset by comparing Fig. 3b for MCV and Fig. 5a, b for the parabolic DPL model with $\chi_0 = 10$.

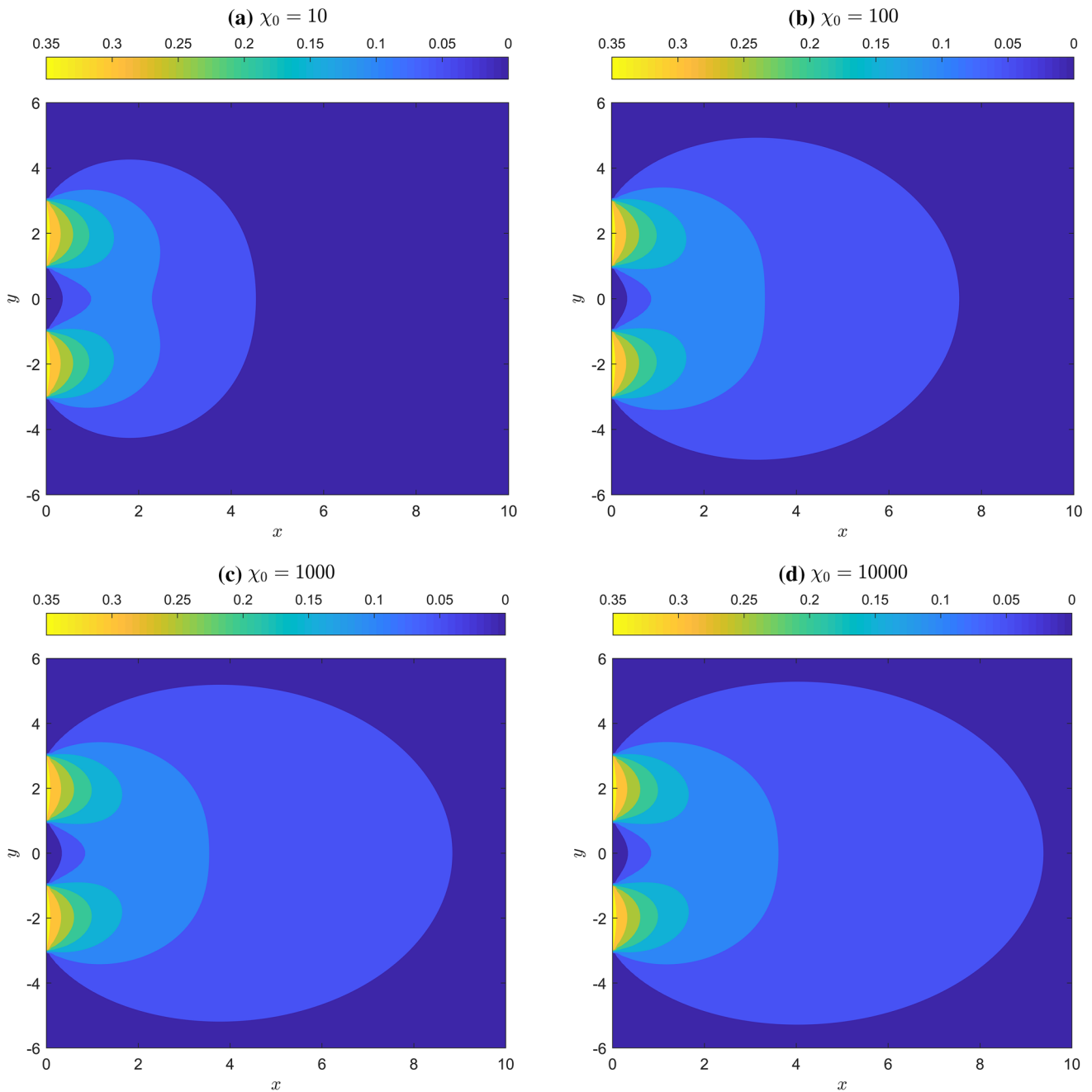


Fig. 8 Effect of the characteristic ratio χ_0 on the propagation of thermal waves governed by the parabolic DPL model with flux-precedence, at dimensionless time $t = 1$

5 Summary

In a summary, we investigated the thermal wave propagation, in a semi-infinite heat conductor, induced by an exponential time-decaying double-strip allowing the waves interference inside the medium. We adopted five models of heat transfer for modeling the thermal propagation and compared the different responses. The five heat transfer models are, respectively, the classical Fourier law, the Maxwell–Cattaneo–Vernotte, the parabolic dual-phase-lag, the hyperbolic dual-phase-lag, and the modified hyperbolic dual-phase-lag. The integral transform technique, based on Laplace–Fourier transform, was employed. An analytical approach based on the solution of two-dimensional problems in the half-space assisted in deriving some analytical and semi-analytical results, refer to (27) and (29). A numerical technique based on the Durbin series and the trapezoidal rule were used to recover the two-dimensional solution in the physical domain. We distinguished the different thermal responses of the half-space conductor under different heat transfer regimes. In the short-time domain, the three hyperbolic heat transfer models were very distinctive with their plane wavefront

which intersects the ground plane xy at the point $x = vt$, where the velocity v is given by Eqs. (32)–(34). We stressed on the Tzou's concepts "flux-precedence" and "temperature-gradient-precedence" and emphasized the validity of these concepts, from a numerical point of view, by monitoring positions of the peaks (the yellow spots) which represent direct indications on such precedence in heat flux or in temperature gradient. The diffusion nature was apparent in both the classical Fourier law and the parabolic dual-phase-lag law, where the wavefront is no longer plane, and its position does not obey the finite speed feature.

We observed the possible wave interference between the two waves resulting from the two strips of the heating boundary condition. The speed of the thermal wave propagation is found to play a key role in the interference onset. The thermal wave speed decreases; the interference occurrence delays.

Funding Open access funding provided by The Science, Technology & Innovation Funding Authority (STDF) in cooperation with The Egyptian Knowledge Bank (EKB).

Data Availability Statement No data associated in the manuscript.

Open Access This article is licensed under a Creative Commons Attribution 4.0 International License, which permits use, sharing, adaptation, distribution and reproduction in any medium or format, as long as you give appropriate credit to the original author(s) and the source, provide a link to the Creative Commons licence, and indicate if changes were made. The images or other third party material in this article are included in the article's Creative Commons licence, unless indicated otherwise in a credit line to the material. If material is not included in the article's Creative Commons licence and your intended use is not permitted by statutory regulation or exceeds the permitted use, you will need to obtain permission directly from the copyright holder. To view a copy of this licence, visit <http://creativecommons.org/licenses/by/4.0/>.

References

- J.B.J. baron Fourier, *Théorie analytique de la chaleur*. Chez Firmin Didot, père et fils, 1822.
- M. Chester, Second sound in solids. *Phys. Rev.* **131**(5), 2013 (1963)
- S.I. Anisimov, B.L. Kapeliovich, T.L. Perel'man, Electron emission from metal surfaces exposed to ultra-short laser pulses. *Sov. Phys. JETP* **39**(2), 375–377 (1974)
- S.D. Brorson, J.G. Fujimoto, E.P. Ippen, Femtosecond electronic heat-transport dynamics in thin gold films. *Phys. Rev. Lett.* **59**(17), 1962–1965 (1987)
- H.E. Elsayed-Ali, T.B. Norris, M.A. Pessot, G.A. Mourou, Time-resolved observation of electron-phonon relaxation in copper. *Phys. Rev. Lett.* **58**(12), 1212–1215 (1987)
- H. Elsayed-Ali, T. Juhasz, G. Smith, W. Bron, Femtosecond thermorefectivity and thermotransmissivity of polycrystalline and single-crystalline gold films. *Phys. Rev. B* **43**(5), 4488 (1991)
- T.Q. Qiu, C.L. Tien, Short-pulse laser heating on metals. *Int. J. Heat Mass Transf.* **35**(3), 719–726 (1992)
- T.Q. Qiu, C.L. Tien, Heat transfer mechanisms during short-pulse laser heating of metals. *ASME J. Heat Transfer* **115**, 835–841 (1993)
- J.K. Chen, J.E. Beraun, Numerical study of ultrashort laser pulse interactions with metal films. *Numer. Heat Transf. A Appl.* **40**(1), 1–20 (2001)
- D.Y. Tzou, *Macro-to microscale heat transfer: The lagging behavior*. 2nd ed. John Wiley & Sons, 2014.
- D.Y. Tzou, Unified field approach for heat conduction from macro- to micro-scales. *J. Heat Transfer* **117**(1), 8–16 (1995)
- E. Awad, On the generalized thermal lagging behavior: Refined aspects. *J. Therm. Stresses* **35**(4), 293–325 (2012)
- D. Jou, M. Criado-Sancho, Thermodynamic stability and temperature overshooting in dual-phase-lag heat transfer. *Phys. Lett. Sect. A Gener. Atom. Solid State Phys.* **248**(2–4), 172–178 (1998)
- S.I. Serdyukov, A new version of extended irreversible thermodynamics and dual-phase-lag model in heat transfer. *Phys. Lett. Sect. A Gener. Atom. Solid State Phys.* **281**(1), 16–20 (2001)
- M. Xu, Thermodynamic basis of dual-phase-lagging heat conduction. *J. Heat Transfer*, **133** (4) (2011)
- R. Quintanilla, R. Racke, A note on stability in dual-phase-lag heat conduction. *Int. J. Heat Mass Transf.* **49**(7–8), 1209–1213 (2006)
- R. Quintanilla, R. Racke, Qualitative aspects in dual-phase-lag heat conduction. *Proc. R Soc. A Math. Phys. Eng. Sci.* **463**(2079), 659–674 (2007)
- S.-N. Li, B.-Y. Cao, Generalized variational principles for heat conduction models based on Laplace transforms. *Int. J. Heat Mass Transf.* **103**, 1176–1180 (2016)
- S.-N. Li, B.-Y. Cao, Approximate analyses of Fourier and non-Fourier heat conduction models by the variational principles based on Laplace transforms. *Numer. Heat Transf. A: Appl.* **71**(9), 962–977 (2017)
- E. Awad, On the time-fractional Cattaneo equation of distributed order. *Physica A* **518**, 210–233 (2019). <https://doi.org/10.1016/j.physa.2018.12.005>
- E. Awad, R. Metzler, Crossover dynamics from superdiffusion to subdiffusion: models and solutions. *Fract. Calculus Appl. Anal.* **23**(1), 55–102 (2020). <https://doi.org/10.1515/fca-2020-0003>
- Y. Povstenko, M. Ostojca-Starzewski, Doppler effect described by the solutions of the Cattaneo telegraph equation. *Acta Mech.* **232**(2), 725–740 (2021)
- K. Górska, Integral decomposition for the solutions of the generalized Cattaneo equation. *Phys. Rev. E* **104**(2), 024113 (2021)
- J.M. Porra, J. Masoliver, G.H. Weiss, When the telegrapher's equation furnishes a better approximation to the transport equation than the diffusion approximation. *Phys. Rev. E* **55**(6), 7771 (1997)
- C. Körner, H. Bergmann, The physical defects of the hyperbolic heat conduction equation. *Appl. Phys. A* **67**(4), 397–401 (1998)
- S.A. Rukolaine, Unphysical effects of the dual-phase-lag model of heat conduction. *Int. J. Heat Mass Transf.* **78**, 58–63 (2014)
- S.A. Rukolaine, Unphysical effects of the dual-phase-lag model of heat conduction: higher-order approximations. *Int. J. Therm. Sci.* **113**, 83–88 (2017)
- E. Awad, Dual-Phase-Lag in the balance: Sufficiency bounds for the class of Jeffreys' equations to furnish physical solutions. *Int J Heat Mass Transf* **158**, 119742 (2020). <https://doi.org/10.1016/j.ijheatmasstransfer.2020.119742>
- E. Awad, T. Sandev, R. Metzler, A. Chechkin, From continuous-time random walks to the fractional Jeffreys equation: Solution and applications. *Int. J. Heat Mass Transf* **181C**, 121839 (2021). <https://doi.org/10.1016/j.ijheatmasstransfer.2021.121839>
- E. Bazhlekova, I. Bazhlekov, Transition from diffusion to wave propagation in fractional Jeffreys-type heat conduction equation. *Fractal Fract.* **4**(3), 32 (2020)
- D.Y. Tzou, The generalized lagging response in small-scale and high-rate heating. *Int. J. Heat Mass Transf.* **38**(17), 3231–3240 (1995)
- K. Hays-Stang, A. Haji-Sheikh, A unified solution for heat conduction in thin films. *Int. J. Heat Mass Transf* **42**(3), 455–465 (1999)

33. W. Troy, M. Dutta, and M. Stroschio, Green's function solutions of one-and two-dimensional dual-phase-lag laser heating problems in nano/microstructures. *J. Heat Transf.* **143** (11) (2021)
34. T.Q. Qiu, T. Juhasz, C. Suarez, W.E. Bron, C.L. Tien, Femtosecond laser heating of multi-layer metals-II. Experiments. *Int. J. Heat Mass Transfer* **37**(17), 2799–2808 (1994)
35. I. Kunadian, J.M. McDonough, K.A. Tagavi, in *Numerical simulation of heat transfer mechanisms during femtosecond laser heating of nano-films using 3-D dual phase lag model*. ASME 2004 Heat Transfer/Fluids Engineering Summer Conference. Charlotte, North Carolina, USA. <https://doi.org/10.1115/HT-FED2004-56823>
36. P. Han, D. Tang, L. Zhou, Numerical analysis of two-dimensional lagging thermal behavior under short-pulse-laser heating on surface. *Int. J. Engng. Sci.* **44**(20), 1510–1519 (2006). <https://doi.org/10.1016/j.ijengsci.2006.08.012>
37. Y. Chou, R.-J. Yang, Two-dimensional dual-phase-lag thermal behavior in single-/multi-layer structures using CESE method. *Int. J. Heat Mass Transf.* **52**(1–2), 239–249 (2009). <https://doi.org/10.1016/j.ijheatmasstransfer.2008.06.025>
38. M.H. Ghasemi, S. Hoseinzadeh, S. Memon, A dual-phase-lag (DPL) transient non-Fourier heat transfer analysis of functional graded cylindrical material under axial heat flux. *Int. Commun. Heat Mass Transf.* **131**, 105858 (2022)
39. W. Dai, R. Nassar, A compact finite difference scheme for solving a three-dimensional heat transport equation in a thin film. *Numer. Methods Partial Differ. Equ.* **16**(5), 441–458 (2000)
40. W. Dai, R. Nassar, A hybrid finite element-finite difference method for solving three-dimensional heat transport equations in a double-layered thin film with microscale thickness. *Numerical Heat Transfer. Part A: Applications* **38**(6), 573–588 (2000)
41. A. Bora, W. Dai, J.P. Wilson, J.C. Boyt, Neural network method for solving parabolic two-temperature microscale heat conduction in double-layered thin films exposed to ultrashort-pulsed lasers. *Int. J. Heat Mass Transfer* **178**, 121616 (2021)
42. D.D. Joseph, L. Preziosi, Heat waves. *Rev. Mod. Phys.* **61**(1), 41–73 (1989)
43. D.D. Joseph and L. Preziosi, Addendum to the paper "heat waves" [Rev. Mod. Phys. 61, 41 (1989)], *Rev. Modern Phys.* **62** (2) (1990) 375–391
44. K.D. Cole, J.V. Beck, A. Haji-Sheikh, and B. Litkouhi, Heat conduction using Green's functions. 2nd ed. *Computational Methods and Physical Processes in Mechanics and Thermal Sciences*, ed. W.J. Minkowycz and E.M. Sparrow. CRC Press, Boca Raton, FL, 2011.
45. A. Erdélyi, W. Magnus, F. Oberhettinger, and F.G. Tricomi, Tables of integral transforms: based in part on notes left by Harry Bateman and compiled by the staff of the Bateman manuscript project. Vol. 1 & 2. McGraw-Hill, New York, 1954.
46. I.H. El-Sirafy, Two-dimensional flow of a nonstationary micropolar fluid in the half-plane for which the shear stresses are given on the boundary. *J. Comput. Appl. Math.* **12**, 271–276 (1985)
47. F. Durbin, Numerical inversion of Laplace transforms: an efficient improvement to Dubner and Abate's method. *Comput. J.* **17**(4), 371–376 (1974)
48. E. Awad, A.R. El Dhaba, M. Fayik, A unified model for the dynamical flexoelectric effect in isotropic dielectric materials. *Eur. J. Mech. A/Solids* **95**, 104618 (2022). <https://doi.org/10.1016/j.euromechsol.2022.104618>
49. G. Honig, U. Hirdes, A method for the numerical inversion of Laplace transforms. *J. Comput. Appl. Math.* **10**(1), 113–132 (1984)
50. H.H. Sherief, K.A. Helmy, A two-dimensional generalized thermoelasticity problem for a half-space. *J. Therm. Stresses* **22**(9), 897–910 (1999)
51. H.H. Sherief, F. Hamza, A. Abd El-Latif, 2D problem for a half-space in the generalized theory of thermo-viscoelasticity. *Mech. Time Depend. Mater.* **19**(4), 557–568 (2015)
52. M.A. Ezzat, E. Awad, Constitutive relations, uniqueness of solution, and thermal shock application in the linear theory of micropolar generalized thermoelasticity involving two temperatures. *J. Therm. Stresses* **33**(3), 226–250 (2010)
53. H.H. Sherief, A.M. Abd-El-Latif, M.A. Fayik, 2D hereditary thermoelastic application of a thick plate under axisymmetric temperature distribution. *Math. Methods Appl. Sci.* **45**(2), 1080–1092 (2022)
54. W.H. Press, S.A. Teukolsky, B.P. Flannery, and W.T. Vetterling, Numerical recipes in Fortran 77: the art of scientific computing. 2nd ed. Vol. 1. Cambridge University Press, 1992.
55. D.-S. Tang, Y.-C. Hua, B.-D. Nie, B.-Y. Cao, Phonon wave propagation in ballistic-diffusive regime. *J. Appl. Phys.* **119**(12), 124301 (2016). <https://doi.org/10.1063/1.4944646>
56. S.A. Rukolaine, A.M. Samsonov, Local immobilization of particles in mass transfer described by a Jeffreys-type equation. *Phys. Rev. E* **88**(6), 062116 (2013)